CONF-791165--3

MASTER

Techniques for the Thermal/Hydraulic Analysis of LMFBR Check Valves

S. M. Cho, Mem. ASME
Manager
Thermal/Hydraulic and Systems Engineering
Nuclear and Advanced Technology Operations
Foster Wheeler Energy Corporation
Livingston, New Jersey 07039

R. S. Kane, Mem. ASME
Assistant Professor
Mechanical Engineering Department
Manhattan College
Riverdale, New York 10471

Abstract

A thermal/hydraulic analysis of the check valves in liquid sodium service for LMFBR plants is required to provide temperature data for thermal stress analysis of the valves for specified transient conditions. Because of the complex three-dimensional flow pattern within the valve, the heat transfer analysis techniques for less complicated shapes could not be used. This paper discusses the thermal analysis techniques used to assure that the valve stress analysis is conservative. These techniques include a method for evaluating the recirculating flow patterns and for selecting appropriately conservative heat transfer correlations in various regions of the valve.

LIST OF SYMBOLS

A_{pfp} = area of a flat plate projected on a cavity, m^2

A_w = total area of cavity walls, m^2

D = inside diameter of a pipe, m

D_i = inner diameter of an annulus, m

D_o = outer diameter of an annulus, m

f = multiplicative factor in equation (11)

g_i = body force per unit mass, $m \cdot s^{-2}$

h = heat transfer coefficient, $W \cdot m^{-2} \cdot {}^{o}C^{-1}$

h_{pfp} = heat transfer coefficient for a flat plate projected onto a cavity, $W \cdot m^{-2} \cdot {}^{o}C^{-1}$

h_w = heat transfer coefficient on a cavity wall, $W \cdot m^{-2} \cdot {}^{o}C^{-1}$

K_i = distributed resistance coefficient, m^{-1}

L = length of entrance region, m

Nu = Nusselt number, dimensionless

Nu_{local} = entrance region Nusselt number, dimensionless

Nu_{∞} = fully developed flow Nusselt number, dimensionless

p = pressure, Pa

Pe = Peclet number, dimensionless

Pr = Prandtl number, dimensionless

q = specific turbulence energy, $m^2 \cdot s^{-2}$

r_i = distributed resistance, $m \cdot s^{-2}$

R_{ij} = Reynolds stress, Pa

u_i, u_j = velocity components, $m \cdot s^{-1}$

x_i, x_j = linear spatial dimension, m

α = factor in correlation (3), dimensionless

LIST OF SYMBOLS (Continued)

α_1 = dissipation coefficient, turbulent parameter in equation (14), dimensionless

β = factor in correlation (3), dimensionless

γ = factor in correlation (3), dimensionless

γ_1, γ_2 = relative diffusivity coefficients, turbulent parameters in equation (15), dimensionless

δ_{ij} = Kronecker delta, dimensionless

ε_M = eddy momentum diffusivity, $m^2 \cdot s^{-1}$

ν = molecular momentum diffusivity, $m^2 \cdot s^{-1}$

ϕ = ratio of heat transfer on a projected flat plate to heat transfer on a cavity wall, dimensionless

$\bar{\psi}$ = average value of the ratio of thermal eddy diffusivity to momentum eddy diffusivity, dimensionless

σ = turbulent kinematic viscosity, $m^2 \cdot s^{-1}$

INTRODUCTION

The Clinch River Breeder Reactor Plant (CRBRP) will be thefirst major U.S. demonstration plant of a large size, liquid metal fast breeder reactor (LMFBR) power plant. Multiple and redundant safeguards against overheating of the reactor are an integral feature of the plant design (1)[1]. The reactor is cooled by liquid sodium in three loops. Each of these three loops in turn transfers the heat removed from the reactor to intermediate loops also carrying liquid sodium. The intermediate sodium loops then transfer this heat to steam/water loops which eventually use the energy obtained to drive a steam turbine and generate electrical power. The sodium coolant passing through the reactor is driven by the action of three primary sodium pumps. Although the three loops are essentially independent, the three coolant streams affect each other in the reactor core itself. In the event of a trip of one of the primary pumps and a loss of flow in that loop, the remaining two operational pumps would tend to reverse the flow of coolant from the idle loop and attempt to drive the tripped pump like a turbine. This cannot be permitted. In order to prevent this from occurring, the system design includes a tilting disc check valve in the cold leg of each of the three primary cooling loops. A failure of the pump in that loop and the resultant inception of reverse flow would cause the check valve disc to move toward a closed position.

[1]Numbers in parentheses refer to the List of References at the end of the paper.

INTRODUCTION (Continued)

Previous work (2) describes the behavior and operation of this type of valve under both forward and reverse flow conditions. This paper describes the heat transfer and related analysis performed to aid the thermal stress analysis of these valves and thereby assure the structural integrity of the valve under a variety of specified transient events.

VALVE DESCRIPTION AND THERMAL STRESS ANALYSIS APPROACH

Figure 1 is a schematic of the CRBRP check valve. Each of the three valves is constructed of type 304 stainless steel and is butttwelded into the 0.610m (24 inch) return piping between the intermediate heat exchanger and the reactor. The valve features a tilting disc which during normal forward flow operation is limited to a maximum open angle of 36° from the vertical. At the lowest normal foward flow, natural circulation in the primary loop, the disc will be located near its free hang angle of 13.4°. Flows lower than the natural circulation flow will occur only if a pump has failed and a flow coastdown toward impending reverse flow is in progress. As the disc approaches its seat, the disc closure from an angle of 6° down to zero is slowed by an orifice-controlled dashpot (the dashpot is not shown in Figure 1). The dashpot is designed to prevent excessively rapid closures and, therefore, to prevent excessively high fluid hammer transient pressures.

The shape of the valve body, the presence of the disc, the location of the dashpot and a large welded access opening with a vent nozzle complicate the flow patterns even during normal foward flow conditions as shown on Figure 1. The flow is straight-through from the inlet piping through the inlet passage leading to the disc. As the flow nears the disc, some of the flow will be

deflected by the disc and form a symmetrical recirculating flow that passes under and then circumferentially around the inlet passage. This flow passes over the top of the disc to rejoin the main flow stream beyond the disc then leaves the valve and enters the downstream piping. The access opening and vent nozzle are welded in place except when removed for repairs and maintenance during shutdown periods. The flow in these areas will be characterized by large, for the access opening, and small, for the vent nozzle, recirculation zones.

The thermal stress analysis of the valve required calculation of heat transfer coefficients and specification of sodium temperatures during certain transient events. Because of the complicated flow patterns in the valve, the thermal analysis of the valve structure was subdivided into smaller regions, each characterized or dominated by one particular type of convective heat transfer mechanism. In those regions where alternative heat transfer mechanisms could be postulated, the most conservative one was used. In general, (with the outside surface of the inlet pipe as a notable exception) the most conservative mechanism was the one that gave the highest heat transfer coefficients and therefore most rapidly transmitted sharp changes in fluid temperature to the valve structure. The task of the structural analysis was then to verify the ability of the valve to withstand a specified number of certain types of thermal cycles. The configuration of the valve suggested that the computerized thermal stress analysis of the valve be performed by subdividing the valve into four major sections. Each section was then considered to be influenced over limited regions, as shown on the Figures 2, 3, 4, and 5, by one type of convective heat transfer mechanism. For specified transients, the convective heat transfer coefficients were supplied for each region.

LINEARIZATION OF TRANSIENT FLOW AND FLUID TEMPERATURE DATA

Prior to the actual analysis, a histogram giving frequency versus severity of transients (as determined by the rate and duration of the most severe temperature change during the event) was developed from the design specification. Similar events in terms of their most severe temperature changes were conservatively placed within a single group that was as severe as the most severe event included in the group. This technique provided a method for evaluating the adequacy of the structure for all specified transients within the framework of an increased frequency but smaller number of separate events. Typically these groups could be characterized as the most severe upshock (rapid increase in temperature), the most severe downshock (rapid decrease in temperature), and the most severe combination of both upshock and downshock.

In order to provide a tractable amount of data for the structural analysis, the curves of sodium temperature and flow rate through the valve as functions of time for specified transient conditions were linearized. The curves were approximated by limited numbers of discrete temperature and flow rate points that if connected by straight lines gave a close description of the actual curve. Portions of the curves characterized by sharp and fluctuating changes in slope within small time spans required closely spaced points. However, many lengthy portions existed where slope changes were infrequent and therefore easily described by widely spaced points. Most of the sharp temperature changes usually occurred within the first 1200 seconds of an event. A typical case required about 20 points for an accurate description.

One characteristic of the transient descriptions was that the points needed to linearize the temperature curve did not generally coincide with the points needed to linearize the flow curve. To simplify the calculation of heat transfer coefficients, the flow curve points alone were used to establish the points for linearized curves of heat transfer coefficient versus time. The temperature variations were considered to have only a secondary

LINEARIZATION OF TRANSIENT FLOW AND FLUID TEMPERATURE DATA (Continued)

effect, through variation of fluid properties, on the value of the local heat transfer coefficients. However the temperature points were considered to be of equal, if not primary importance, in the input to the structural analysis work. Therefore both linearized sets of data, heat transfer coefficients versus time based on the linearized flow curves, and the fluid temperature versus time were supplied. The preponderant effect of flow on heat transfer coefficient as compared to that of temperature permitted the structural analysis to safely interpolate linearly in the heat transfer coefficient data to obtain coefficients corresponding to the linearized temperature data points.

HEAT TRANSFER CORRELATIONS

Table 1 lists the heat transfer correlations used for the regions shown on Figures 2 through 5. (Most of the correlations cited in the table were taken from Reference (3) which provides an excellent collection of liquid metal heat transfer information.) Correlation (1) is obtained from a solution for fully developed turbulent flow in a pipe. This situation does not occur anywhere within the valve where a pipe flow correlation is most appropriate. The flow into the valve is disturbed by the presence of an elbow only about 6 diameters upstream of the valve inlet. Consequently, the heat transfer coefficients based on correlation (1) were modified using correlation (2) which accounts for the effects of developing flow.

The region around the outside of inlet passage is subject to both a reverse axial flow and a circumferential flow (the analysis used to determine the velocity distribution in this region is described later). A conservative stress analysis in this region results from the use of the heat transfer correlation that gives the lowest reasonable heat transfer coefficient. The combination of a high heat transfer coefficient on the inside of the inlet passage and a lower heat transfer coefficient on the outside of the inlet passage increases the

TABLE 1: HEAT TRANSFER CORRELATIONS

CORRELATION	APPLICABLE REGION		REF. NO.
	FIG. NO.	REGION NO.	
(1) $Nu_\infty = 5.0 + 0.025Pe^{0.8}$	(2)	(1)	(3)
	(3)	(3,4,5,6)	
(2) $Nu_{local} = 1.72(\frac{D}{L})^{0.16} \cdot Nu_\infty$	(2)	(1)	(4)
	(3)	(3,4,5,6)	
(3) $Nu = \alpha + \beta(\bar{\psi}Pe)^{\gamma}$ where $\alpha = 4.82 + 0.697(\frac{D_o}{D_i})$, $\beta = 0.0222$, $\gamma = 0.758(\frac{D_o}{D_i})^{0.053}$, $\bar{\psi} = 1 - \frac{1.82}{Pr(\varepsilon_M/\nu)^{1.4}_{max}}$	(2)	(2,4,6)	(3)
(4) $Nu = 4.98 + 0.662(\frac{D_o}{D_i})$	(2)	(2,4,6)	(3)
(5) $Nu = 0.42Pe^{0.65}$	(2)	(7)	(4)
	(3)	(1,2)	
	(4)	(1,2)	
	(5)	(1)	
(6) $Nu = 1.13Pe^{0.5}$	(2)	(3,5)	(3)
(7) $h_w = h_{pfp} \frac{1}{\phi} \frac{A_{pfp}}{A_w}$	(4)	(3)	(5)
	(5)	(2,3)	
(8) $Nu = 5.0$	(5)	(3)	(3)
(9) $h = 0$	(2)	(8,9,10)	—
	(3)	(7,8,9)	
	(4)	(4,5,6,7,8,9,10,11,12)	
	(5)	(4,5,6)	
(10) $Nu = a + fb(\bar{\psi}Pe)^c$	(2)	(11)	—

transient thermal stresses across the wall during periods of rapidly varying fluid temperatures. The correlation that was used for the outside of the inlet passage, correlation (3), satisfies the criteria for the conservative stress analysis. Correlation (3) is appropriate for annular flow, using the reverse axial velocities, and gives lower heat transfer coefficients than any reasonable correlation that might have been used for the somewhat higher circumferential velocities in this region. In correlation (3), the hydraulic diameter of an annulus was used as the characteristic dimension in the Nusselt and Peclet numbers. The momentum diffusivity ratio (ε_M/ν) appearing in this correlation is a function of Reynolds number and geometry. Curves suitable for design calculations appear in Reference 3. The theoretical background and derivation of relationships for the momentum diffusivity ratio are given in Reference(9). If the thermal-to-momentum diffusivity ratio, $\bar{\psi}$, became negative, the ratio was set equal to zero. For some very low flow rates, the Nusselt number obtained from correlation (3) was calculated to be lower than would exist by molecular conduction alone. In those cases correlation (4), which was derived from the basic heat transfer equations for molecular conduction only, was used.

Correlation (5) was used to evaluate the heat transfer coefficients in regions where the flow was better described as flow over a flat plate rather than flow in a pipe. This was the case near regions of a recirculating flow where circumferential flow was expected. The Nusselt and Peclet numbers were then based on an estimate of the average path length of a circumferential flow along the valve wall. This technique gave conservatively high values for the heat transfer coefficient.

Correlation (6) was used to evaluate the heat transfer coefficients over the sides of the seat ring surface. Because of the flow recirculation in this region, a conservative estimate for the coefficient is obtained by assuming that reverse axial flow here behaves similarly to flow over a sphere. On these

surfaces, as indicated earlier for the outer surface of the inlet passage itself, a conservative stress analysis results if the lowest reasonable value of heat transfer coefficient is chosen. The combination of rapid response on the inner pipe surface and a slower response on the outer pipe surface provides a more severe loading condition for the thermal stress analysis. The characteristic length for correlation (6) was taken as the outer diameter of the seat ring.

Correlation (7) was used to evaluate heat transfer coefficients where stationary recirculation regions were expected as in the access opening and in the vent nozzle. The flat plate coefficients needed in correlation (7) were obtained from correlation (5). The area ratio, as suggested in Reference (5), was considered a reasonable approximation for a mixing length ratio required for the correlation. The heat transfer ratio, ϕ, required in correlation (7) was obtained from a curve of the heat transfer ratio versus mixing length ratio given in Reference (5). For the smaller vent nozzle opening, there existed the possibility that molecular conduction alone would give a higher coefficient than the convective correlation. Correlation (8) was used to check this possibility. The heat transfer regions listed in Table 1 for correlation (9) represented the outer, insulated surface of the valve or arbitrary breaks between valve model subdivisions. In these regions, the heat transfer coefficient was set equal to zero (adiabatic boundary condition). Correlation (10) was used for the edge of the inlet passage. As discussed below, the coefficient in this region was evaluated by treating it as a rearward facing step in the entrance region of a pipe. In application to this heat transfer region, correlation (10) became identical to correlation (1) as modified by correlation (2) when f=1 and $\bar{\gamma}=1$.

Because of the complex geometry that might be seen in future valve designs, a more general approach may be used to develop liquid metal correlations from more common liquid (non-metal) heat transfer correlations. It is noted that

liquid metal correlations are typically of the form:

$$Nu = a + b(\bar{\psi}Pe)^c \qquad (10)$$

The first term on the right hand side of this equation represents a molecular conduction contribution for a liquid metal that is not normally seen in a non-metallic liquid correlation. The second term represents the turbulent eddy contribution which is normally seen in a non-metallic liquid correlation. One may reason that the enhancement or reduction, seen in the heat transfer of a non-metallic liquid from flow disturbances should also be seen in similar proportion in a liquid metal if only the hydrodynamic part of the liquid metal correlation is considered. Although the liquid metal has vastly different conduction properties, its hydrodynamic behavior in turbulent flow and the effect of flow disturbances is not greatly different from that seen with more typical liquids. One can therefore modify equation (10) to appear as:

$$Nu = a + fb(\bar{\psi}Pe)^c \qquad (11)$$

The multiplicative factor f can be used to modify known liquid metal correlations, if the effect of a flow disturbances on the basic flow pattern, for example a pipe bend in a generally straight pipe, is known from ordinary liquid studies.

The technique of using multiplicative factors to develop correlations from a basic flow pattern for a disturbed flow pattern has been successfully used before. Reference (6) uses this procedure to give the factor f for a curved pipe in terms of the radius of curvature, pipe radius, and Reynolds Number. Although the example cited (6) provides a multiplicative factor for friction, this can be extended to that part of the liquid metal Nusselt number correlation that depends on hydrodynamics alone. Similar multiplication factors for cavities and forward and rearward facing steps may be found in References (10), (11), and (12). The same concept can also be used for a surface with protrubulences. It should be noted that the factor $\bar{\psi}$ in equation (11) accounts for the effect of

HEAT TRANSFER CORRELATIONS (Continued)

differing thermal and momentum eddy diffusivities for liquid metals and has been retained in equation (11). The factor f would account only for flow pattern disturbances which in ordinary liquid correlations have similar effects on both heat transfer and friction. Therefore either friction or heat transfer data for disturbed flows of ordinary liquids could be used to evaluate the factor f. A frequently encountered example of this technique is in the evaluation of heat transfer in a cavity or near steps where f typically is of the order of 0.5. In the analyses described previously for the access opening and for the vent nozzle an available closed form correlation was used, except for the edge of the inlet passage (Region 1' of Figure 2) where f was taken to be 1.0 in order to give a conservatively high heat transfer coefficient due to additional turbulances created by the presence of the disc assembly.

SODIUM FLOW DISTRIBUTION

A modified version of a computer program, known as VARR-II (7) capable of handling turbulent flows was used to evaluate the portion of the flow that recirculates around and over the inlet flow passage after striking the disc. The computer program uses a numerical method to calculate multi-dimensional, axisymmetric, time-dependent, turbulent flows with small density variations. The solution technique is based on the simplified marker-and-cell (SMAC method. It allows for a variety of initial and boundary conditions as well as arbitrarily placed internal obstacles. The program has been used previously to evaluate velocity distributions in the CRBRP-IHX (8).

SODIUM FLOW DISTRIBUTION (Continued)

VARR-II provides a solution to the finite difference formulation of the governing equations for an incompressible turbulent flow. The governing equations, in differential form, are:

$$\frac{\partial}{\partial x_j} u_j = 0 \tag{12}$$

$$\frac{\partial u_i}{\partial t} + \frac{\partial}{\partial x_j}(u_i u_j) = -\frac{1}{\rho}\frac{\partial p}{\partial x_i} + g_i - \frac{1}{\rho}\frac{\partial}{\partial x_j}(R_{ij}) \tag{13}$$

$$\frac{\partial q}{\partial t} + \frac{\partial}{\partial x_j}(u_j q) = \frac{1}{2}\sigma\left(\frac{\partial u_i}{\partial x_j} + \frac{\partial u_j}{\partial x_i}\right)^2 + \frac{\partial}{\partial x_j}\left(\gamma_1 \sigma \frac{\partial q}{\partial x_j}\right) - \alpha_1 \frac{(2q)^2}{\sigma} \tag{14}$$

$$\frac{\partial \sigma}{\partial t} + \frac{\partial}{\partial x_j}(u_j \sigma) = \frac{\sigma^2}{4q}\left(\frac{\partial u_i}{\partial x_j} + \frac{\partial u_j}{\partial x_i}\right)^2 + \frac{\sigma}{q}\frac{\partial}{\partial x_j}\left(\gamma_1 \sigma \frac{\partial q}{\partial x_j}\right) - \frac{\sigma^3}{q^2}\frac{\partial}{\partial x_j}\left[\gamma_2 q \frac{\partial}{\partial x_j}\left(\frac{q}{\sigma}\right)\right] - \alpha_1 q \tag{15}$$

$$R_{ij} = \frac{2}{3}\rho q \delta_{ij} - \rho\sigma\left(\frac{\partial u_i}{\partial x_j} \cdot \frac{\partial u_j}{\partial x_i}\right) \tag{16}$$

The double subscript tensor notation has been used in equations (12) through (16) where a repeated j indicates summation over all three values of j. Although shown in cartesian form, the program will handle a cylindrical coordinate system by internally modifying the equations to the appropriate form.

Equation (12) is the continuity equation for an incompressible fluid. Equation (13) is the unsteady momentum equation. In the finite difference formulation of equation (13), an additional distributed resistance term, r_i defined as:

$$r_i = K_i \frac{u_i 2}{2} \tag{17}$$

is included. This term is necessitated by the cellular description of the flow field and the possible presence of solid obstacles within individual flow cells. This term would not be present if infinitesimally small cell sizes could be used

around any solid obstacles. In that extreme case, the equations would reduce to the original differential form and solid obstacles would become boundary conditions. In the finite difference formulation, only the overall boundaries of the cellular grid are treated as boundary conditions. Local obstacles are included within the flow field.

Equations (14) and (15) provide a two-equation, three-parameter model of the turbulence. Equation (14) describes the distribution of turbulent kinetic energy while equation (15) describes the variation of the turbulent kinematic viscosity. Equation (16) defines the Reynolds stress terms of equation (13).

The VARR-II analysis of the check valve was done in two parts. The flow field in the recirculation region around the inlet flow passage was calculated first. The velocities calculated from this model were used as input to a second model for the flow field downstream of the inlet passage. The disc in this model was treated as a local obstacle. In the recirculation region analysis, it was assumed, as would be expected, that the major velocity components are circumferential and axial. In the downstream model, the major velocity components were assumed to be radial and axial.

Figure 6 shows averages of calculated circumferential and axial velocities for the recirculation region model. These velocities give a recirculation of about 35% of the total flow into the valve. A less sophisticated approach based simply on the equivalence of pressure losses for the recirculating and straight-through flow path to the exit of the valve gave a recirculation of about 30%. In this second approach, each right angle turn in a postulated flow path was assumed to have the same loss coefficient regardless of whether the flow path was in the main or recirculating flow stream. The slightly higher recirculation of the computer program was used to evaluate the heat transfer coefficients.

SODIUM FLOW DISTRIBUTION (Continued)

In the recirculation region, the average circumferential velocities are larger than the axial velocities. This tendency weakens as the recirculation region ends beyond the seat ring. As explained previously in evaluating the most conservative heat transfer coefficients, these results were considered in generally choosing annular correlations based on axial velocities in the recirculation region for the outside surface of the inlet pipe and flat plate correlations further downstream for the inside surface of the valve body. The velocities in Figure 6 are based on full design flow into the valve. The highly turbulent nature of the flow suggested that a Reynolds number invariance was a reasonable description as Reynolds numbers greater than 1,000,000 in the inlet pipe were typical, even at low flows. It was therefore assumed that the flow distribution was similar for lower inlet flows and that local velocities decreased linearly with decreases in the inlet velocity. Provided that Reynolds numbers are very large, Reynolds number invariance can also be used for other valve geometries to realistically justify use of a known flow distribution to evaluate local and average velocities at flow rates other than the one used to develop the known distribution.

At full flow, heat transfer coefficients ranged from as high as 29,200 $W \cdot m^{-2} \cdot {}^{o}C^{-1}$ (5136 BTU/hr -ft^2-^{o}F) in Region 1 of the inlet assembly to as low as 1870 $W \cdot m^{-2} \cdot {}^{o}C^{-1}$ (330 BTU/hr-ft^2-^{o}F) in Region 6C of the inlet assembly (Figure 2). Regions with high coefficients, such as Region 1, had values decrease by as much as 80% because of large decreases in flow rate during some of the transients considered. Regions with initially low coefficients, such as Region 6C mentioned above, could not undergo such large variations since molecular conduction provided a uniform lower bound on the size of the coefficient.

SUMMARY

An approach to the problem of evaluating heat transfer coefficients in the complex geometry of an LMFBR check valve has been presented. The correlations used to calculate the coefficients were based on a realistic assessment of the

SUMMARY (Continued)

flow patterns within the valve. Where choices between correlations were considered, the correlation that yielded results giving a more conservative thermal stress analysis was chosen.

ACKNOWLEDGEMENT

This paper is based partly on work supported by the U.S. Department of Energy under Westinghouse-Advanced Reactors Division Contract No. 54-7CCY-199282 and Foster Wheeler Energy Corporation Contract No. 8-33-2752. The authors thank the members of the valve project team at Foster Wheeler Energy Corporation for their contribution to this work.

LIST OF REFERENCES

1. Anon, "Clinch River Breeder Reactor Plant Project, Design Description", Breeder Reactor Corporation, CRBRP-PMC-77-06, Oak Ridge, Tennessee 37830.

2. Kane, R. S., and Cho, S. M., "Hydraulic Characteristics of Tilting-Disc Check Valves", Journal of the Hydraulic Division, American Society of Civil Engineers, Vol. 102, No. HY1, January 1976, pp. 57-72.

3. Dwyer, O.E., Liquid Metal Heat Transfer , Brookhaven National Laboratory, BNL 11936R, January 1969.

4. Kutateladze, S. S., et. al., Liquid Metal Heat Transfer Media, Supplement No. 2 of the Soviet Journal of Atomic Energy, Translated by Consultants Bureau, Inc. of N. Y., Chapman and Hall, Ltd. London, 1959.

5. Fenton, L., and White, R. A., "Heat Transfer in Resonant Cavities Spanned by Low Speed, Turbulent Shear Layers", Journal of Basic Engineering, Trans. of American Society of Mechanical Engineers, Vol. 93, September 1971, pp. 455-457.

6. Ito, H., "Friction Factors for Turbulent Flow in Curved Pipes", Journal of Basic Engineering, American Society of Mechanical Engineers, June 1959, pp. 123-134.

7. Cook, J. L., and Nakayama, P. I., "VARR-II, A Computer Program for Calculating Time Dependent Turbulent Fluid Flows with Slight Density Variation", Westinghouse Electric Corporation, Advanced Reactors Division, Report No. WARD-D-0106, Madison, Pennsylvania, 1975.

8. Aburomia, M. M., Chan, B. C., and Cho, S. M., "Flow Distribution Analysis in Nuclear Heat Exchangers with Application to CRBRP-IHX" Proceedings of the 1976 Heat Transfer and Fluid Mechanics Institute, Stanford University Press, 1976.

9. Dwyer, O. E., "Eddy Transport in Liquid-Metal Heat Transfer", A.I.Ch.E. Journal, Vol. 9, No. 2, March 1963, pp. 261-268.

10. Charwat, A. F., Dewey, C. F., Roos, J. N., and Hitz, J. A., "An Investigation of Separated Flows - Part II: Flow in the Cavity and Heat Transfer", Journal of the Aerospace Sciences, Vol. 28, No. 7, July 1961, pp. 513-527.

11. Saki, N., Fukusako, S., and Hirata, T., "Laminar Heat Transfer Downstream of a Sudden Enlargement of a Duct", Bulletin of the J.S.M.E., Vol. 21, No. 152, February 1978, pp. 254-257.

12. Chilcott, R. E., "A Review of Separated and Reattaching Flows with Heat Transfer", Int. J. of Heat and Mass Transfer, Vol. 10, 1967, pp. 783-797.

LIST OF FIGURE CAPTIONS

Figure 1. Primary Loop, Cold Leg Check Valve

Figure 2. Inlet and Seat Assembly, Heat Transfer Regions

Figure 3. Outlet Assembly, Heat Transfer Regions

Figure 4. Access Penetration Assembly, Heat Transfer Regions

Figure 5. Vent Nozzle Assembly, Heat Transfer Region

Figure 6. Recirculation Zone, Average Velocities at Full Design Flow

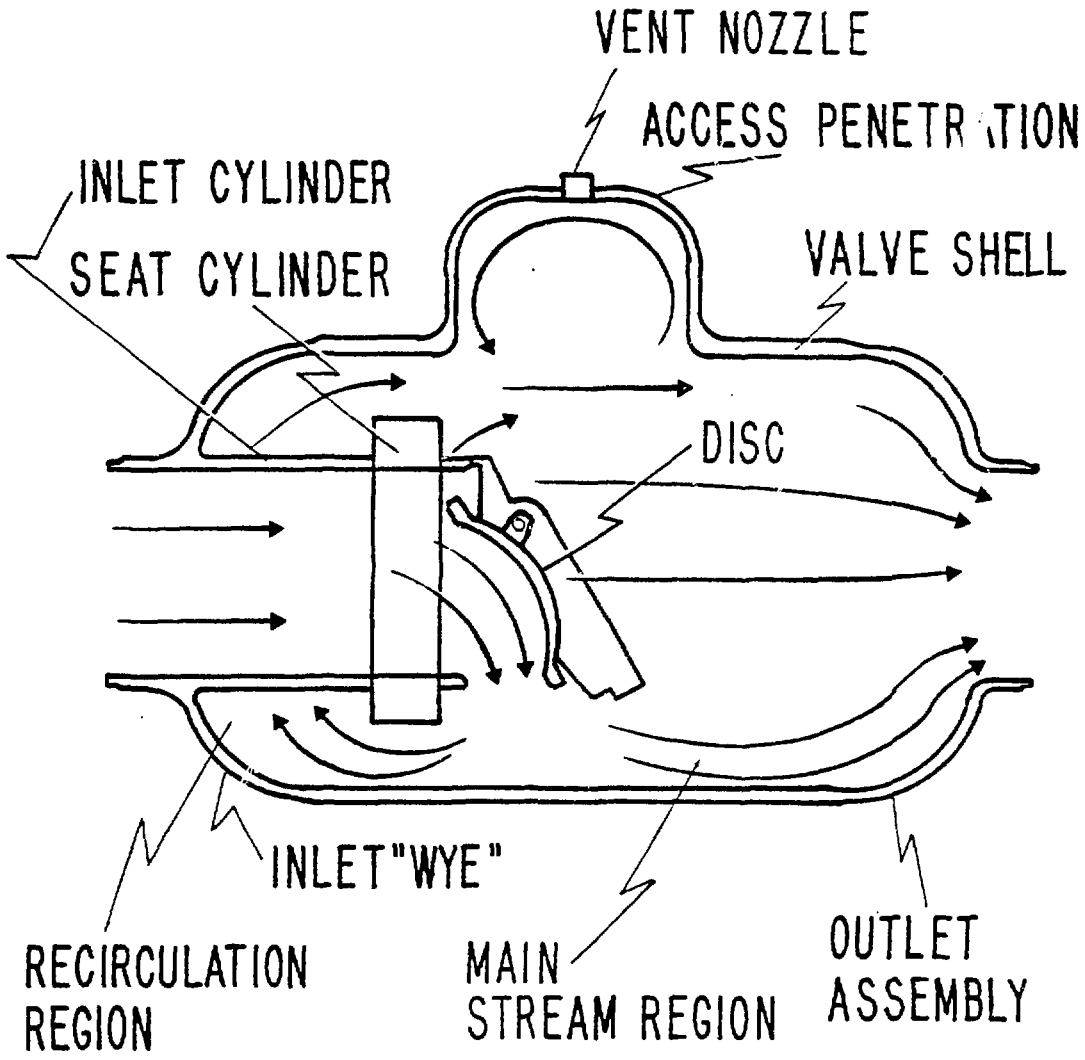

FIGURE 1. PRIMARY LOOP, COLD LEG CHECK VALVE

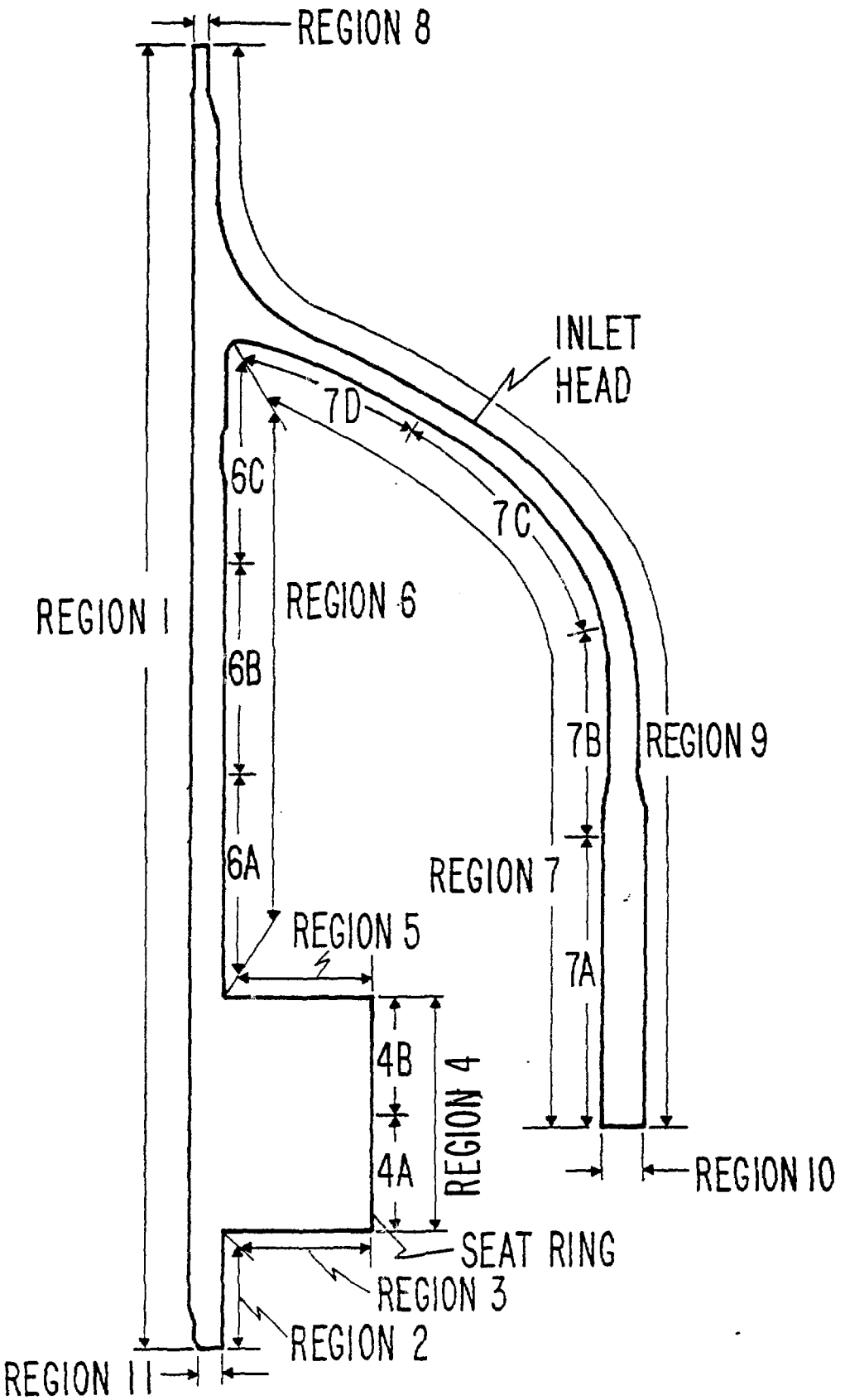

FIGURE 2. INLET AND SEAT ASSEMBLY, HEAT TRANSFER REGIONS

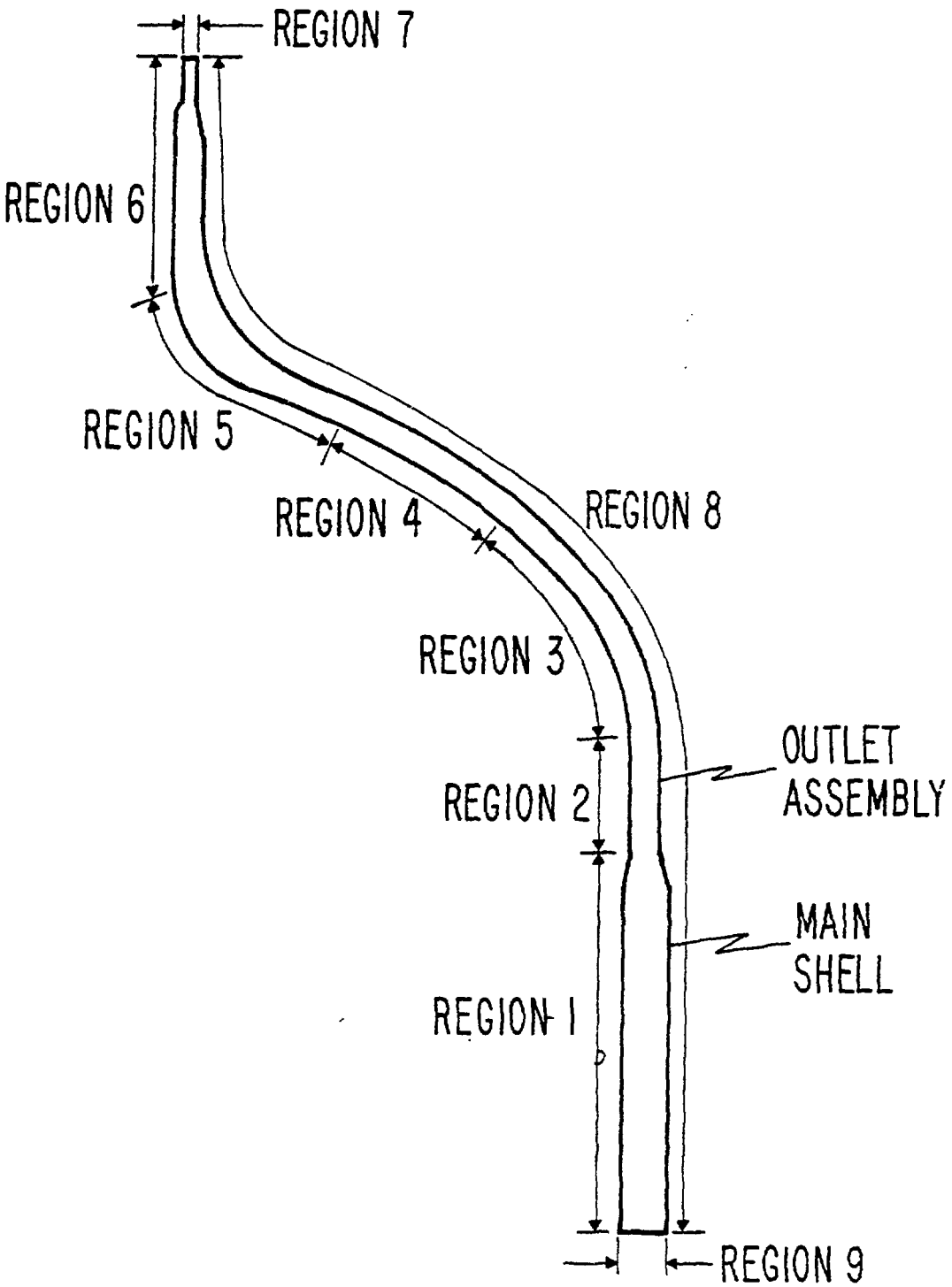

FIGURE 3. OUTLET ASSEMBLY, HEAT TRANSFER REGIONS

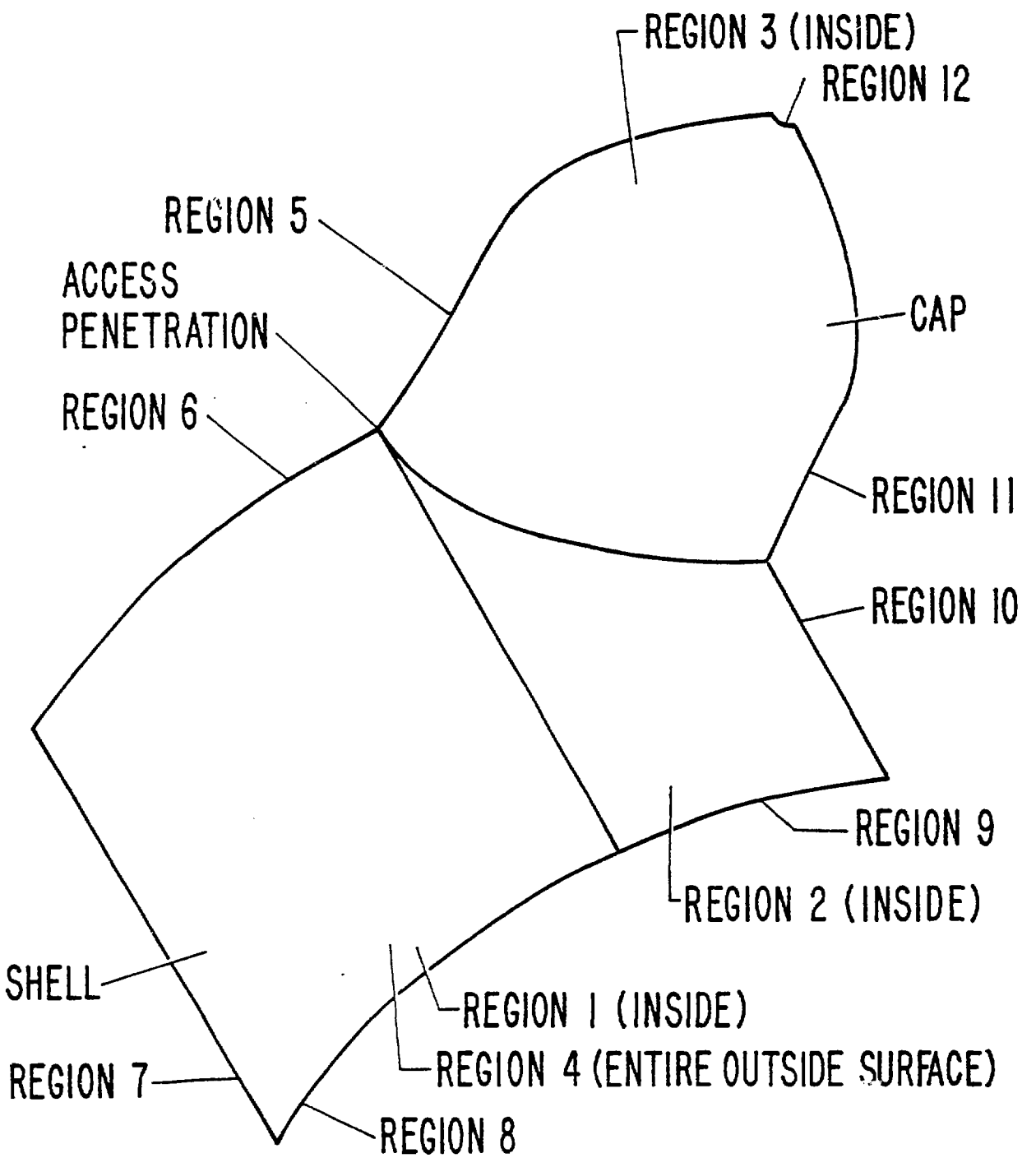

FIGURE 4. ACCESS PENETRATION ASSEMBLY, HEAT TRANSFER REGIONS

CH2-KTNE

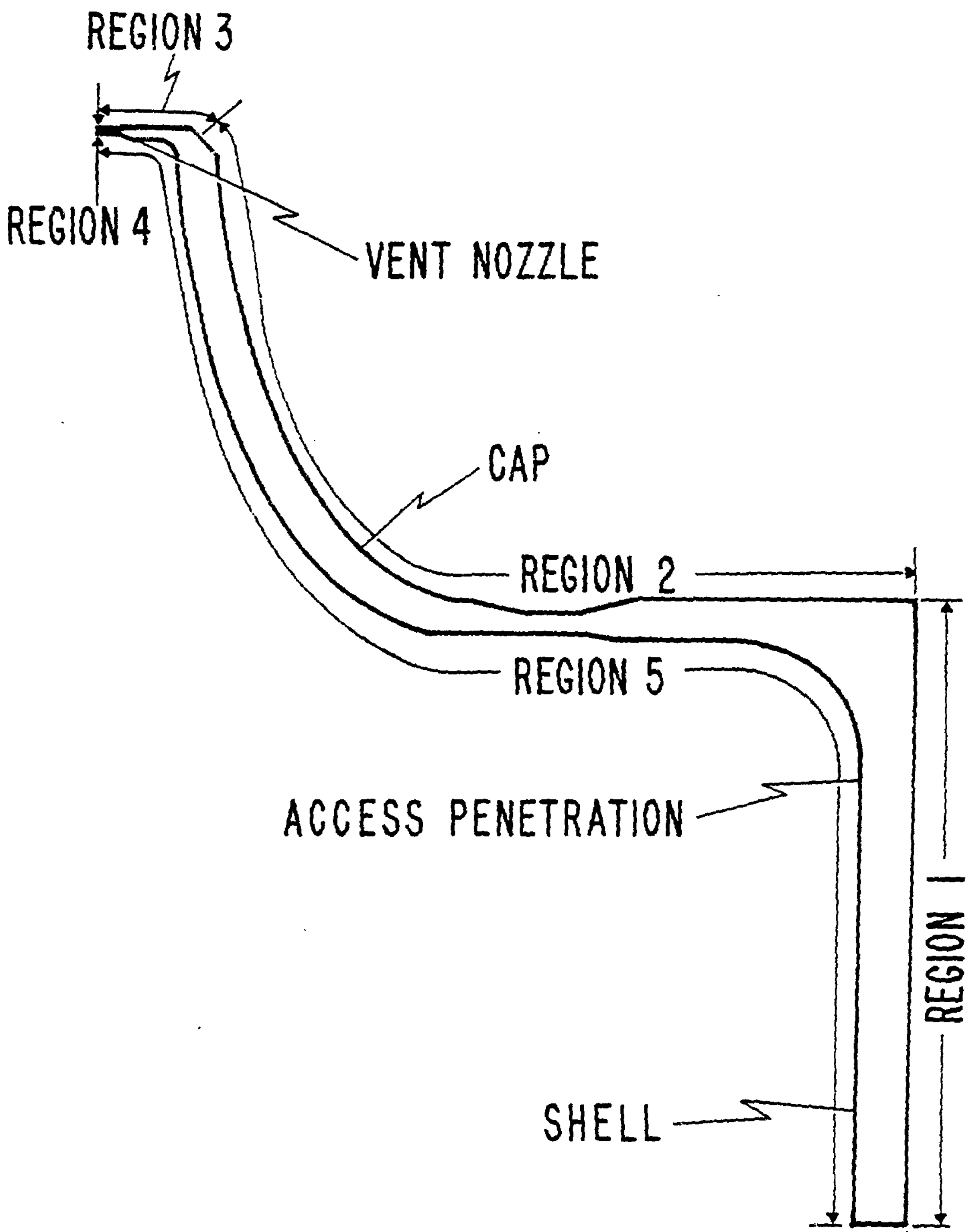

FIGURE 5. VENT NOZZLE ASSEMBLY, HEAT TRANSFER REGIONS

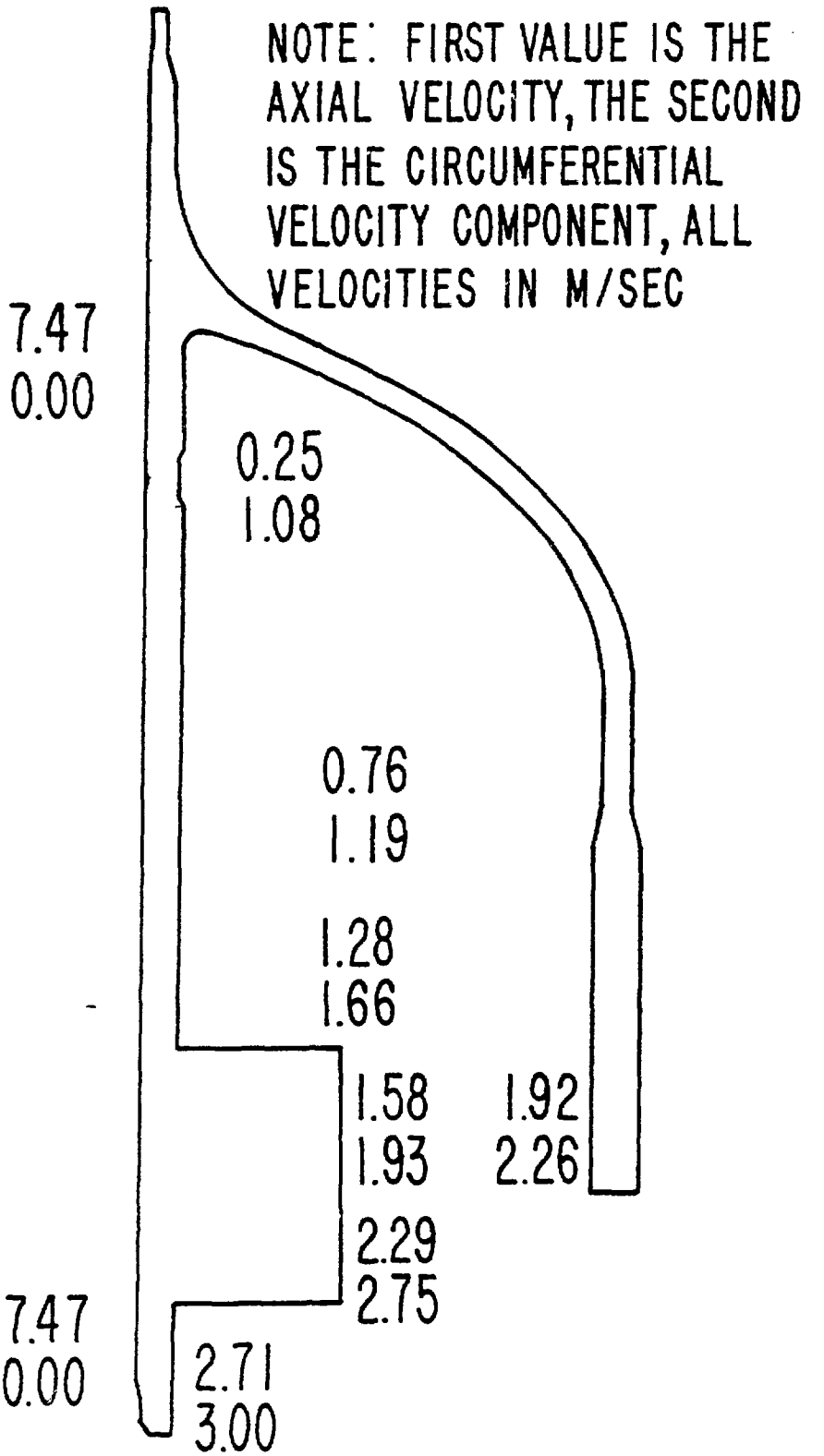

FIGURE 6. RECIRCULATION ZONE, AVERAGE VELOCITIES AT FULL DESIGN FLOW